X-ray spectral variations of U Gem from quiescence to outburst

T. Güver,[1][*] C. Uluyazı,[1] M. T. Özkan[2] and E. Göğüş[3]

[1]*Istanbul University, Science Faculty Department of Astronomy & Space Sciences, Istanbul 34119, Turkey*
[2]*Istanbul University, University Observatory, Istanbul 34119, Turkey*
[3]*Sabancı University, Faculty of Engineering and Natural Sciences, 34956 Istanbul, Turkey*

ABSTRACT

In this paper, we report the discovery of a high-energy component of the X-ray spectra of U Gem, which can be observed while the source is in outburst. We used *Chandra* and *XMM–Newton* observations to compare the quiescence and outburst X-ray spectra of the source. The additional component may be the result of the reflection of X-rays emitted from an optically thin plasma close to the white dwarf, from the optically thick boundary layer during the outburst. Another possible explanation is that some magnetically channelled accretion may occur on to the equatorial belt of the primary causing shocks similar to the ones in the intermediate polars as it was suggested by Warner and Woudt. We have also found a timing structure at about 73 mHz ($\sim$13.7 s) in the *RXTE* observation, resembling dwarf novae oscillations.

Key words: binaries: close – stars: dwarf novae – stars: individual: U Gem – novae, cataclysmic variables – X-rays: stars.

1 INTRODUCTION

Dwarf novae are highly variable mass-exchanging binary star systems containing a white dwarf and a late-type K or M star. They are characterized by occasional outburst episodes which typically take place on a time-scale of 100 d and last for about 15 d. Outbursts are believed to be triggered by a thermal instability in the accretion disc that drives the disc from a low-temperature, low mass-accretion rate, quiescent state to a hot, high-$\dot{m}$ outburst state.

About every 120 d prototypical dwarf nova U Gem exhibits outbursts, where the *V* magnitude of the system rises from $\sim$14 to $\sim$9 (Szkody & Mattei 1984). During outbursts U Gem is a bright extreme ultraviolet (EUV) source. This emission is interpreted as optically thick radiation from a $\sim$140 000 K boundary layer (Long et al. 1996). Besides, there is observational evidence that the observed energy from the boundary layer and that from the disc is comparable (Long et al. 1996) which is in accordance with the simple mass-accretion scenario (Pringle 1977). In quiescence the UV spectra of U Gem is dominated by the white dwarf emission as observed with *IUE* (Kiplinger, Sion & Szkody 1991), Hopkins Ultraviolet Telescope (HUT) (Long et al. 1993) and *Hubble Space Telescope* (*HST*) (Long et al. 1994). Studies of the white dwarf in U Gem indicate evidence for an equatorial accretion belt (Cheng et al. 1997; Long et al. 1993) which is cooling during the quiescence interval.

X-ray emission (0.2–10 keV) has been observed from U Gem both in quiescence and in outburst (Swank et al. 1978; Cordova & Mason 1984; Szkody et al. 1996). Unlike other well-known dwarf novae systems, such as SS Cygni, hard X-ray flux of U Gem does not decrease in outbursts (Mattei, Mauche & Wheatley 2000). The fact is that the increase in the hard X-ray (2–15 keV) flux is less than that of the soft X-ray flux (0.1–4 keV; Cordova & Mason 1984; Mattei et al. 2000). *Chandra* observations of U Gem in quiescence indicate that the hard X-ray emission arises from a gas with a small scaleheight ($< 10^7$ cm) close to the white dwarf (Szkody et al. 2002, hereafter S02).

Here, we present detailed hard X-ray emission properties of U Gem in outburst phase for the first time. We find an extra non-thermal X-ray component arising during outburst which can be interpreted as a sign of a transient magnetosphere occurring in the boundary layer of U Gem as a result of the increase of the mass-accretion rate (Warner & Woudt 2002).

In Section 2, we present observations and our data analysis. In Sections 3 and 4, we show observational differences between quiescence and outburst phases, respectively. In Section 5, we discuss these results.

2 OBSERVATIONS AND DATA ANALYSIS

We use four pointed observations of U Gem with three satellites, namely *Chandra*, *XMM–Newton* (Jansen et al. 2001) and *RXTE*. These observations enable us to study both the outburst and the quiescence states of the source. Details of these observations can be found in Table 1. We should note that although both outbursts are normal outbursts, the outburst in 2004 is a few days longer than the outburst in 2002. Second *Chandra* observation was made during the peak of a normal outburst in 2002 (see Fig. 1), while in 2004, a series of *RXTE* observations were made in order to cover the whole outburst. Time of the *Chandra* X-ray observation is marked on the AAVSO data of the outbursts in Fig. 1.

[*]E-mail: tolga@istanbul.edu.tr

Table 1. Details of all U Gem observations used in this study.

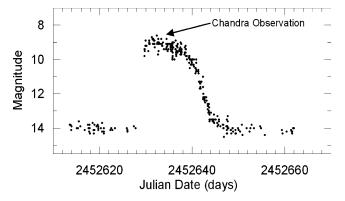| Satellite	Obs ID	Approximate exposure (ks)	Instrument/grating	Start time (UT)	Source state
Chandra	647	100	ACIS-S/HETG	2000-11-29 12:00:17	Quiescence
XMM	0110070401	23	All	2002-05-09 10:46:06	Quiescence
Chandra	3767	67	ACIS-S/HETG	2002-12-26 09:27:36	Outburst
RXTE	80011-01	115	PCA	2004-02-27 12:49:54	Outburst

Figure 1. AAVSO light curve of the optical outburst in 2002. The arrow marks the time of *Chandra* observation.

In the public data archive of *Chandra*, there are three observations of U Gem with a total approximate exposure time of 217 000 s. For this study, however, we will not present the LETG observation since we will be interested mainly on the high-energy X-ray emission of the source. *Chandra* data were analysed by *Chandra* Interactive Analysis of Observations [1] software version 3.2 and *Chandra* Calibration Data base (CALDB) version 3.0.0. A new bad pixel file was created to identify and flag hot pixel and afterglow events in ACIS observations. This tool searches for pixels where the bias value is too low or too high, classifies the events on suspicious pixels as being associated with cosmic ray afterglows, hot pixels or astrophysical sources and adds newly found bad pixels to the output new bad-pixel file. The first *Chandra* observation, while the source was in a quiescence state, was reported in detail by S02.

For the extraction of the scientific information from the *XMM–Newton* data, XMM-SAS version 6.1 and the latest available calibration files were used. We used EPPROC, EMPROC meta tasks to extract calibrated source events. Since we will be interested in mainly the high-energy part of the spectrum, we will not be presenting RGS data, which were presented by Pandel et al. (2005).

RXTE pointed observations of U Gem were performed between 2004 February 27 and March 14, with a total effective exposure time of 115 ks. Onboard *RXTE*, there are two main instruments: the Proportional Counter Array (PCA), an array of five nearly identical proportional counter units (PCU) that are sensitive to photon energies between 2 and 60 keV, and the High Energy X-ray Timing Experiment (HEXTE) that is sensitive 20–200 keV photons. In this study, we only used data collected with the PCA. For each *RXTE* observation, we extracted spectrum using the Standard2 data collected with PCU2 since it was operational in all the 24 *RXTE* pointings.

The background spectrum for each pointing was obtained using the PCA background models for bright sources.

We have used XSPEC v11.2 (Arnaud 1996) for the analysis of continuum spectra. In order to use chi square analysis we have grouped all spectra to have at least 40 counts in each bin. Since we have high-enough count rates in grating spectra, we did not try to fit the zero-order ACIS spectra, therefore we did not have to model the pile-up effects of the ACIS CCDs which was also mentioned in S02 for the quiescence data. Because of the difference in the responses of detectors, we took different energy ranges for different data sets, for *Chandra* gratings we used 0.5–7.0 and 0.8–7.5 keV energy range for medium energy grating (MEG) and high energy grating (HEG), respectively, and for the *XMM–Newton* EPIC-PN (Turner et al. 2001) data we used the 0.2–10 keV region.

3 QUIESCENCE

During quiescence, we have two observations of U Gem from two different satellites. We simultaneously model X-ray spectra from these pointings assuming that the system was in the same X-ray regime during these observations, as it was the case for the optical emission (∼14 mag). We fit the spectrum with the so-called XSPEC models cemekl or cvmekl. These models assume an optically thin plasma cooling from a maximum temperature that follows a power-law distribution. The only difference between the cemekl and cvmekl models is that the latter one calculates the abundances of all elements with respect to the solar values, and the former one calculates these values for 13 most abundant elements separately. An application of this model and a more detailed discussion can be found in Pandel, Cordova & Howell (2003). With a little worse χ_ν^2 value, we could also fit the spectrum with another XSPEC model mkcflow which was also used for cataclysmic variables (CVs) by Mukai et al. (2003). Our results for the quiescence state are presented in Table 2 and the spectra can be seen in Fig. 2. For the calculation of N_H and abundances we used XMM EPIC-PN and *Chandra* MEG data as a reference to the other data sets. From the narrow lines in the *Chandra* spectra of U Gem in quiescence, a low-velocity emission region close to the white dwarf was suggested by S02.

4 OUTBURST

One of the interesting properties of the X-ray spectra during outburst is the broadened emission lines, for the quiescence phase properties of the X-ray emission lines have been studied in S02 and from the measured broadening of the lines it has been suggested that the lines originate from a low-velocity material instead of an inner disc region rotating at the Keplerian velocity. From the investigations of the quiescent spectra, narrow X-ray emission lines appear to be a common situation for some other CVs also. However, outburst X-ray spectrum of U Gem shows that most of the emission-line fluxes are increased and most of them are broadened. To be able to

[1] CIAO, http://cxc.harvard.edu/ciao/

Table 2. Best-fitting model parameters for quiescence. Uncertainties are calculated for 90 per cent confidence interval. Fluxes are calculated for the given energy ranges of the data sets. Abundance values are fixed to the value obtained from MEG fit. N_H values are fixed to the value obtained from EPIC-PN fit.

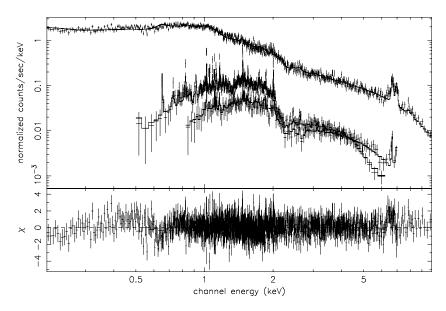| Data set	Model name	N_H (10^{20} atoms cm^{-2})	T_{max} kT (keV)	Power-law index α	$\dot{m}$ (10^{-12} gr yr^{-1})	Flux (10^{-11} erg cm^{-2} s^{-1})	Abundance ($\odot$)	χ_ν^2
HEG	cemekl	–	22.47 ± 7.15	0.96 ± 0.27	–	1.15 ± 0.05	–	1.006
MEG	cemekl	–	23.22 ± 7.70	1.05 ± 0.14	–	1.05 ± 0.03	1.30 ± 0.22	1.006
EPIC-PN	cemekl	0.98 ± 0.26	29.25 ± 4.36	0.87 ± 0.06	–	0.78 ± 0.02	–	1.006
HEG	mkcflow	–	28.41 ± 3.80	–	6.64 ± 0.36	1.14 ± 0.1	–	1.093
MEG	mkcflow	–	35.08 ± 2.78	–	5.42 ± 0.15	1.16 ± 0.04	1.31 ± 0.10	1.093
EPIC-PN	mkcflow	0.47 ± 0.19	27.49 ± 0.96	–	4.77 ± 0.06	1.17 ± 0.02	–	1.093

Figure 2. Best-fitting model to all observations of U Gem during quiescence.

Table 3. Properties of the emission lines, which were observed during both quiescence and outburst, are given. All the line detections were made by Medium Energy Grating, MEG, onboard *Chandra*. Velocities of the lines are not corrected to the orbital inclination of the system. Errors for some of the lines velocities are not given because these lines are modelled by fixing the FWHM value to 0.023 Å which is the limit for MEG.

Line	Wavelength (Å)	Quiescence flux (10^{-5} photons cm^{-2} s^{-1})	Outburst flux (10^{-5} photons cm^{-2} s^{-1})	Quiescence velocity (km s^{-1})	Outburst velocity (km s^{-1})
S xv	5.0665	0.94 ± 0.52	4.16 ± 1.47	1350	4180 ± 2000
Si xiv	6.1804	2.17 ± 0.33	6.91 ± 0.80	1120	3080 ± 460
Mg xii	8.4192	1.86 ± 0.27	2.59 ± 0.49	820	2200 ± 690
Mg xi	9.1687	0.70 ± 0.26	1.26 ± 0.62	552 ± 277	2000 ± 900
Fe xxiv	10.6190	2.14 ± 0.43	4.89 ± 0.96	1340 ± 440	4450 ± 1000
Ne x	12.1321	3.46 ± 0.65	11.2 ± 1.85	1000 ± 290	3450 ± 550
Fe xvii	15.0140	3.17 ± 0.89	12.3 ± 2.49	740 ± 350	2470 ± 760
O viii	16.0055	1.14 ± 0.70	3.98 ± 1.87	430	1400 ± 1200
Fe xvii	17.0510	2.97 ± 1.10	17.9 ± 3.96	400	2830 ± 913

make a comparison, in Table 3 we have given a summary of some of the emission lines detected in both observations of *Chandra*.

In order to model the emission lines, listed in Table 3, we first fit the local region of a line with a polynomial function so that the continuum can be estimated. We than add a Gaussian to fit the residuals from the continuum. ATOMDB data base is used for the identification of the lines, and the calculation of the velocities is done by assuming, the measured full width at half-maximum

(FWHM) values of the emission lines arise only because of the Doppler broadening of the material in a Keplerian orbital motion around the white dwarf.

Interestingly, we find excess high-energy component (as seen in the upper panel of Fig. 3) in the outburst spectra when fitted with the model adequately represent the quiescence spectrum. This did not fit the data neither with the frozen model parameters (except flux, which was found as $\sim 3.08 \times 10^{-11}$ erg cm^{-2} s^{-1}) found from
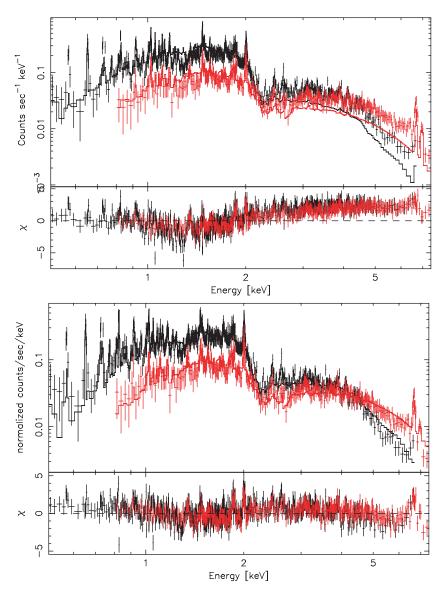
Figure 3. Outburst spectra fitted with the cemekl model. Upper panel shows the results when the best-fitting parameters for the quiescence is used. Lower panel presents the results when a power-law model is added to the cemekl model.

Table 4. Best-fitting model parameters for only outburst. Uncertainties are calculated for 90 per cent confidence interval. Abundance is also fixed to 1.05 solar. Additional model is power law whose photon index is given with the Γ. N_H values are fixed to the value obtained from MEG fit.

Data set	Model name	N_H $(10^{21}$ atoms cm$^{-2})$	T_{max} kT (keV)	Power-law index of cemekl α	Photon index Γ	T (keV)	Flux $(10^{-11}$ erg cm^{-2} s$^{-1})$	χ^2_ν
MEG	cemekl	0.37 ± 0.004	100 ± 3.4	0.52 ± 0.04	–	–	3.00	1.877
HEG	cemekl	0.37 ± 0.004	100 ± 13.2	0.69 ± 8.23	–	–	3.40	1.877
HEG	cemekl+pow	0.45 ± 0.45	9.49 ± 4.1	1.35 ± 0.49	0.54 ± 0.16	–	3.31 ± 1.38	1.297
MEG	cemekl+pow	0.45 ± 0.45	18.44 ± 10.5	0.26 ± 0.11	0.64 ± 0.06	–	3.39 ± 0.53	1.297
HEG	cemekl+bremss	3.43 ± 0.38	94.17	0.07	–	199.3	–	–
MEG	cemekl+bremss	3.43 ± 0.38	1.73	0.01	–	199.3	–	–

the quiescence phase analysis ($\chi^2_\nu \sim 2.95$) (see the upper panel of Fig. 3) nor with allowing the parameters to vary ($\chi^2_\nu \sim 1.877$), which also gave physically unacceptable values (see Table 4).

In order to resolve this, we fixed the cemekl model parameters as obtained from quiescence and added a power-law component to this

model. In this way, we could obtain an acceptable fit with a χ^2_ν value of 1.41. Then we set the parameters to be free which reduced the χ^2_ν even further to 1.3. Results of these fits are given in Table 4, and the spectra can be seen in the bottom panel of Fig. 3. We have also tried some other models, such as thermal-bremmstrahlung, which

gave either unphysical results or unacceptable χ^2_ν values. Just for presentation, these results are given in Table 4.

We have also analysed all individual *RXTE*/PCA spectra obtained during the 2004 outburst. We fitted the background-subtracted PCA spectrum in 3–20 keV range with a thermal (cemekl) plus power-law model but fixing the parameters of the thermal component at the values obtained from *Chandra* observations in 2002. As a result, we find that the hard X-ray spectral shape of U Gem varies significantly throughout the 2004 outburst; in 14 of 23 spectra, a power-law model with indices between 0.28 and 1.34 was needed to successfully fit the data, while in nine of 23 spectra, no power-law component was required. This trend provides evidence for transient spectral changes in U Gem during the outburst episode. However, it is crucial to note that the PCA response does not allow to constrain the low-energy (thermal) component, and the projected *Chandra* spectral shape in 2002 may not reflect the intrinsic spectral shape in 2004. To conclusively quantify the high-energy spectral variations, simultaneous wide band X-ray observations are needed.

4.1 Quiescent subtracted spectrum

In order to investigate the difference in the spectral properties of the quiescence and outburst phases more reliably we have employed the following technique. We assumed the spectrum of the quiescent phase as that of the background for the outburst spectrum so that the remaining spectral information would be only due to spectral changes in the source during outburst.

For the fitting, we could not use the lower energies because, when subtracted, count rates of these regions were too low to make a reliable fit so we have used 1.0–6.5 keV and 1.0–7.0 keV range for MEG and HEG, respectively.

Resultant spectrum can be best fitted by a power law with a χ^2_ν value of 0.98. By only fitting a power law to the subtracted data, the change in the X-ray emission lines can also be clearly seen which have more flux and are apparently broader than in quiescent state. In order to investigate the origin of the difference and to fit the emission lines, we have also tried some other XSPEC models like the derivatives of the mekal models and bremss model; these fittings gave either very bad χ^2_ν values or unphysical results. Results are given in Table 5 and the spectrum can be seen in Fig. 4.

4.2 Timing analysis

To examine the timing characteristics of the hard X-ray emission from U Gem during the 2004 February and March outburst, we performed a standard timing analysis as follows. We generated the 2–15 keV light curves with time binning of 16 ms using the PCA event mode data and converted the times to the solar system barycenter. For each *RXTE* pointing, we divided light curves into 512 s long

segments. We then applied Fourier transformation to each of 512 s data segment and computed associated Fourier (Leahy) powers. We obtained the power spectrum of each pointing by averaging the Fourier power spectra of all available segments.

We find that the power spectra were dominated by red noise structure below about 10 mHz and consistent with powers due to Poisson count fluctuations at frequencies above. We determine that the rms amplitudes of low-frequency fluctuations vary in the range of 1.2 and 7.3 per cent. Interestingly, we detect a quasi-periodic timing structure in the *RXTE* observations on 2004 March 13. The power spectral density of this pointing is shown in Fig. 5. We fitted the power spectrum with the sum of a constant, a power law and a Lorentzian function to account for the Poisson noise, low-frequency red noise and the quasi-periodic oscillations (QPO) structure, respectively. For the QPO feature, we obtain the peak frequency as 73 ± 9 mHz and rms amplitude as 1.0 ± 0.3 per cent. The peak frequency of this oscillation corresponds to 13.7 s.

5 DISCUSSION

In this work, we have investigated U Gem's X-ray behaviour during outburst. We found that unlike quiescence, one cannot fit the X-ray spectrum of U Gem with a simple mekal-based multitemperature spectral model. Instead, an additional non-thermal component, most likely a power law, is needed. We should also note that when fitting the excess hard X-ray emission with a power law, deviations from the continuum can be seen (see Figs 4 and 3). We think that these deviations arise because of the broadening and increase of the fluxes of the X-ray emission lines when compared to the quiescence phase. In order to be able to obtain better fits to the outburst data, one should also be able to model the broadening of the lines physically, which is currently unavailable.

Interpretation of the extra X-ray component can be made as follows. Since this component was observed only during outburst phase, there must be a mechanism which is temporarily available in outbursts. During quiescence, the mass-accretion rate is not enough to create an optically thick boundary layer, but in outbursts there is observational evidence for such a boundary layer (Long et al. 1996). Comparing the X-ray spectra obtained in quiescence and outburst, we see that the optically thin plasma observed in quiescence can also be seen in outburst with approximately the same temperature, but there exists an additional spectral component. Reflection of this X-ray emitting plasma from the optically thick boundary layer might occur in outburst giving rise to the extra X-ray component. Such reflection models are applied to active galactic nuclei; furthermore a similar detection for reflection during an outburst was reported by Done & Osborne (1997) for SS Cygni. According to the reflection scenario, besides this extra component, one would expect to see Kα fluorescent lines (Beardmore et al. 1995; Done et al. 1995) due to

Table 5. Results of the modelling of the quiescence subtracted spectra. Model is power law. Fluxes are calculated for the 1.0–7.0 keV range, because of low signal-to-noise ratio below 1 keV. N_H is frozen to the value obtained from N_H calculator of HEASARC.

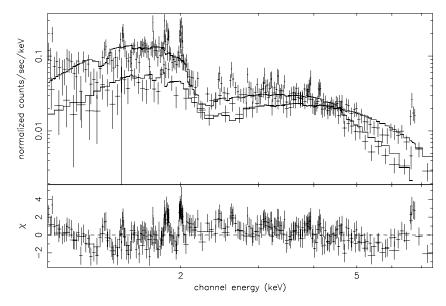| Data set	Model name	T_{max} (keV)	Photon index Γ	Flux (10^{-11} erg cm^{-2} s^{-1})	χ^2_ν
MEG	pow	–	0.46 ± 0.06	2.42 ± 0.14	1.02
HEG	pow	–	0.67 ± 0.08	2.25 ± 0.26	1.02
MEG	mekal	79.89 ± 3.40	–	1.50 ± 0.03	1.68
HEG	mekal	79.89 ± 5.11	–	1.98 ± 0.05	1.68
MEG	bremss	199.4 ± 15.2	–	1.52 ± 0.01	1.62
HEG	bremss	199.4 ± 23.8	–	1.98 ± 0.01	1.62

Figure 4. Quiescent subtracted, outburst spectra and the best-fitting model cemekl+pow.

the reflection of hard X-rays from the relatively cold EUV emitting boundary layer. Unfortunately, in the high-resolution *Chandra* spectra of U Gem during outburst those lines are either very weak or absent especially when compared to the resonance lines of Fe apparent near 1.86 Å. Moreover, such reflection components are most effectively seen as a bump around 20 keV (Done & Osborne 1997).

Another plausible explanation for this hard X-ray component arises with the help of low inertia magnetic accretor model (LIMA; Warner & Woudt 2002). According to the model, during outbursts the spin-up of an accretion belt of the weakly magnetic white dwarf will enhance the intrinsic magnetic field and with this way, magnetically channelled accretion can occur even on low-field CV primaries. With such an accretion on to the equatorial belt of the primary, accretion curtains and shocks in the same manner as in the standard intermediate polar structure are possible (Warner & Woudt 2002). This model is useful for explaining the dwarf nova oscillations (DNOs) observed in outbursts. In this model these DNOs are interpreted as the pulsations at the rotation period of this transient magnetosphere.

As we have noted above, an equatorial accretion belt has been deduced from UV observations (Long et al. 1993; Cheng et al. 1997). So, if accretion curtains and shocks are likely to occur in U Gem during outbursts then a thermal bremsstrahlung or a power-law-like emission may be observed from the cooling post-shock gas showing us an extra X-ray component. From the *Chandra* observations in quiescence (S02) and *HST* observations during outburst (Sion et al. 1997), it has been suggested that magnetic accretion is possible for U Gem.

We find a significant structure in one power spectrum that is similar to QPO. This feature appears around 73 mHz ($\sim$13.7 s). Transient DNOs have been observed for U Gem, during outbursts, in the 25 s range, by *EXOSAT* (Mason et al. 1988) and *EUVE* (Long et al. 1996). These oscillations may be arising from the transient magnetosphere which is predicted by the LIMA model. We, therefore, suggest that the extra X-ray spectral component as well as transient QPO we detected originates from a transient magnetosphere.

Another issue is the apparent changes in the emission-line profiles, whose some of the properties are summarized in Table 3. Increase in the fluxes can be understood by assuming a high-mass
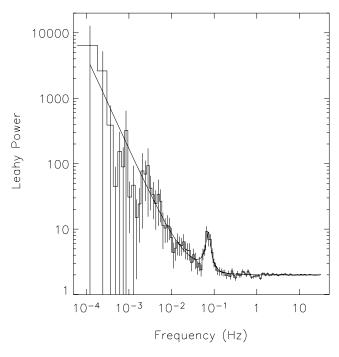

Figure 5. Power spectrum of the PCA data obtained on 245 3077 JD, a QPO structure can be seen near 73 mHz.

transfer to the inner disc during outburst. This will increase the probability of collisions between particles, which will of course increase collisional ionization. However, broadening of the lines cannot be explained that easily. We can assume that during the outbursts outer parts of the accretion disc move towards the white dwarf and the emission lines come from a region rotating with Keplerian velocities. Although this idea is mainly in agreement with the standard outburst theories (Warner 1995), it is not obvious from only one observation, because there are still some lines which are not as broadened as expected to form in a region rotating with a Keplerian velocity.

In order to understand this phenomenon, further broad-band observations of U Gem as well as other CVs are needed to investigate

the overall variations, particularly in the boundary layer, between the quiescence and outburst phases.

REFERENCES

Arnaud K. A., 1996, in Jacoby G., Barnes J., eds, ASP Conf. Ser., Vol. 101, Astronomical Data Analysis Software and Systems V. Astron. Soc. Pac., San Francisco, p. 17
Beardmore A. P., Done C., Osborne J. P., Ishida M., 1995, MNRAS, 272, 749
Cheng F. H., Sion E. M., Horne K., Hubeny I., Huang M., Vrtilek S. D., 1997, AJ, 114, 1165
Cordova F. A., Mason K. O., 1984, MNRAS, 206, 879
Done C., Osborne J. P., Beardmore A. P., 1995, MNRAS, 276, 483
Done C., Osborne J. P., 1997, MNRAS, 288, 649
Jansen F. et al., 2001, A&A, 365, L1
Kiplinger A. L., Sion E. M., Szkody P., 1991, ApJ, 366, 569
Long K. S., Blair W. P., Bowers C. W., Davidsen A. F., Kriss G. A., Sion E. M., 1993, ApJ, 405, 327
Long K. S., Sion E. M., Huang M., Szkody P., 1994, ApJ, 424, 49
Long K. S., Mauche C. W., Raymond J. C., Szkody P., Mattei J. A., 1996, ApJ, 469, 841
Mason O. K., Cordova F. A., Watson M. G., King A. R., 1988, MNRAS, 232, 779
Mattei J. A., Mauche C., Wheatley P. J., 2000, JAVSO, 28, 160
Mukai K., Kinkhabwala A., Peterson J. R., Kahn S. M., Paerels F., 2003, ApJ, L586, 77
Pandel D., Cordova A., Howell S. B., 2003, MNRAS, 346, 1231
Pandel D., Cordova F. A., Mason K. O., Priedhorsky W. C., 2005, ApJ, 626, 396
Patterson J. Raymond J. C., 1985, ApJ, 292, 535
Pringle J. E., 1977, MNRAS, 178, 195
Sion E. M. et al., 1997, ApJ, 483, 907
Swank J. H., Boldt E. A., Holt S. S., Rothschild R. E., Serlemitsos P. J., 1978, ApJ, 226, 133
Szkody P. Mattei J. A., 1984, PASP, 96, 988
Szkody P., Long K. S., Sion E. M., Raymond J. C., 1996, ApJ, 469, 834
Szkody P., Nishikida K., Raymond J. C., Seth A., Hoard D. W., Long K., Sion E. M., 2002, ApJ, 574, 942 (S02)
Turner M. J. et al., 2001, A&A, 365, L27
Warner B., 1995, Cataclysmic Variable Stars. Cambridge Univ. Press, Cambridge
Warner B., Woudt P. A., 2002, MNRAS, 335, 84

This paper has been typeset from a TEX/LATEX file prepared by the author.